Cell size has pervasive effects on the functional composition and morphology of leaves: a case study in *Rhododendron* (Ericaceae)

Arezoo Dastpak[1,2], Monica Williams[3], Sally Perkins[4], John A. Perkins[3], Charles Horn[5], Patrick Thompson[6], Connor Ryan[7], Juliana Medeiros[7], Yi-Dong An[8], Guo-Feng Jiang[8], Kevin A. Simonin[9], Adam B. Roddy[2,10] *

[1] Department of Biology, Faculty of Basic Science, Central Tehran Branch, Islamic Azad University, Tehran, Iran

[2] Institute of Environment, Department of Biological Sciences, Florida International University, Miami, FL, USA

[3] Azalea Society of America, Washington, D.C., USA

[4] American Rhododendron Society, Great River, New York, USA

[5] Department of Biology, Newberry College, Newberry, SC, USA

[6] Davis Arboretum, Auburn University, Auburn, AL, USA

[7] Holden Forests and Gardens, Kirtland, OH, USA

[8] State Key Laboratory of Conservation and Utilization of Subtropical Agrobioresources and Guangxi Key Laboratory of Forest Ecology and Conservation, College of Forestry, Guangxi University, Nanning, Guangxi, China

[9] Department of Biology, San Francisco State University, San Francisco, CA, USA

[10] current address: Department of Environmental Studies, New York University, New York, NY, USA

***Correspondence**
Adam B. Roddy,
Email: adam.roddy@nyu.edu

Edited by J. Torres-Ruiz

Abstract

The leaf economics spectrum (LES) characterizes a tradeoff between building a leaf for durability versus for energy capture and gas exchange, with allocation to leaf dry mass per projected surface area (LMA) being a key trait underlying this tradeoff. However, regardless of the biomass supporting the leaf, high rates of gas exchange are typically accomplished by small, densely packed stomata on the leaf surface, which is enabled by smaller genome sizes. Here, we investigate how variation in genome size-cell size allometry interacts with variation in biomass allocation (i.e. LMA) to influence the maximum surface conductance to CO_2 and the rate of resource turnover as measured by leaf water residence time. We sampled both evergreen and deciduous *Rhododendron* (Ericaceae) taxa from wild populations and botanical gardens, including naturally occurring putative hybrids and artificially generated hybrids. We measured genome size, anatomical traits related to cell sizes, and morphological traits related to water content and dry mass allocation. Consistent with the LES, higher LMA was associated with slower water residence times, and LMA was strongly associated with leaf thickness. Although anatomical and morphological traits varied orthogonally to each other, cell size had a pervasive impact on leaf functional anatomy: for a given leaf thickness, reducing cell size elevated the leaf surface conductance and shortened the mean water residence time. These analyses clarify how anatomical traits related to genome size-cell size allometry can influence leaf function independently of morphological traits related to leaf longevity and durability.

1-Introduction

Leaves play a central role in whole-plant strategies for resource acquisition and growth, thereby impacting ecosystem function and climate (Bazzaz et al. 1987; Boyce and Lee 2010; Bonan et al. 2014; Franks et al. 2017). Quantifying the diversity of leaf structural organizations and their coordination with carbon gain and plant growth has, therefore, been a central goal in plant functional ecology (Chapin 1989; Poorter et al. 1990; Reich et al. 1992; Wright et al. 2004; Violle et al. 2007; Reich 2014). One example, the leaf economics spectrum (LES), identifies a suite of coordinated leaf traits considered to be the result of natural selection acting to optimize the balance between the lifetime carbon costs

of leaf construction and maintenance and the carbon gain from photosynthetic metabolism (Reich et al. 1992; Kikuzawa and Lechowicz 2006, 2011; Kikuzawa and Lechowicz 2018). One of the key traits used to quantify the tradeoff between resource allocation toward building a leaf for durability and longevity as opposed to energy capture and gas exchange is specific leaf area (SLA) or its reciprocal, leaf dry mass per unit projected surface area (LMA) (Wright et al. 2004). The underlying premise behind the positive relationship between LMA and leaf life span (LL) is that, as LMA increases, more resources are dedicated to investment in durability instead of photosynthesis. This results in lower photosynthetic capacity per unit biomass (Westoby et al. 2013; Osnas et al. 2013; Lloyd et al. 2013). Thus, species with low LMA possess a high photosynthetic capacity per unit leaf mass (A_{mass}) and short LL (i.e. fast resource turnover), whereas species with high LMA possess a low A_{mass} and long LL (i.e. slow resource turnover). Although coordination between LMA, LL, and A_{mass} is observed across terrestrial plant species globally, the utility of LMA to predict A_{mass} or LL varies substantially between plant groups and is particularly weak among deciduous species (Wright et al. 2004; Poorter et al. 2009). This has led to a re-examination of LES traits and the broader physiological and structural constraints on leaf architecture (Onoda et al. 2017).

Fluxes of CO_2 and water between plants and the atmosphere are typically calculated per unit leaf surface area. However, the turnover times of matter that scale with leaf longevity and whole-plant relative growth rate depend not only on the mass supporting a given leaf surface area but also on the structure of the leaf volume supplied by its surface area (Roderick et al. 1999a, 1999b; Shipley et al. 2006; Théroux-Rancourt et al. 2023). The development of the LES has incorporated total leaf volume insofar as leaf mass per area increases with leaf thickness (Shipley 1995; Poorter et al. 2009; De La Riva et al. 2016). However, leaf thickness (T_{L}) is only one component of LMA and may account for a small fraction of interspecific variation in LMA (Witkowski and Lamont 1991; Shipley 1995; De La Riva et al. 2016; John et al. 2017). Furthermore, although thinner leaves have the potential for greater energy and matter exchange per unit leaf volume (i.e. they have a higher ratio of surface area to volume), realizing this potential would require a high conductance to CO_2, which is achieved by having smaller cells (Franks and Beerling 2009;

de Boer et al. 2012; Simonin and Roddy 2018; Roddy et al. 2020; Théroux-Rancourt et al. 2021). Thus, both leaf morphology (T_L) and anatomy (cell size) influence rates of energy and matter exchange, and they can vary independently of each other (Figure 1). Additionally, because metabolic processes occur in an aqueous environment, photosynthetic capacity is affected not only by the rates of CO_2 diffusion into the leaf but also by leaf water content (Roderick et al. 1999a, 1999b; Huang et al. 2020; Théroux-Rancourt et al. 2021; Borsuk et al. 2022; Wang et al. 2022). While a thick leaf would have higher water content and a higher potential photosynthetic capacity per unit projected leaf surface area than a thin leaf, a thick leaf would typically have lower potential photosynthetic capacity per leaf volume. Furthermore, at constant leaf surface conductance, increasing leaf thickness would increase leaf water content per leaf area and slow leaf water turnover.

Here, we test how morphological and anatomical traits influence leaf functional anatomy using a group of closely related *Rhododendron* species. The genus *Rhododendron* encompasses >1000 species globally, spanning temperate and tropical biomes, and exhibits diversity in leaf habitat (deciduous and evergreen) as well as variation in genome size and ploidy (Schepper et al. 2001; Jones et al. 2007; De et al. 2010; Shrestha et al. 2018; Khan et al. 2021; Hu et al. 2023). We sampled broadly among *Rhododendron*, including species growing in botanical gardens and naturally occurring plants from wild populations. We also include co-occurring, putative interspecific and interploidy hybrids, as well as artificially generated interploidy hybrids. Because genome size is often correlated with cell size (Beaulieu et al. 2008; Roddy et al. 2020; Théroux-Rancourt et al. 2021; Jiang et al. 2023), we used variation in genome sizes among *Rhododendron* to tease apart the effects of cell size and leaf morphology on functional leaf anatomy. We predicted (1) that morphological traits (lamina thickness, LMA, leaf water content) would be correlated with each other as predicted by the LES but largely independent of variation in anatomical traits (e.g. cell sizes and packing densities), and (2) that although anatomical and morphological traits would be independent of each other, cell size variation would nonetheless influence correlations among leaf thickness, metabolic capacity, and the turnover times of water. Testing these hypotheses helps clarify the various ways that cells, tissues, and whole leaves

can be built and the potential effects of variation at different levels of organization on leaf ecological strategies.

2-Methods

2.1-Rhododendron diversity and plant material

In total, we measured 148 *Rhododendron* accessions (accessioned material in botanical gardens or wild-growing plants). For 15 of the naturally occurring deciduous azaleas (section Pentanthera), we resampled the same individuals in years 2022 and 2023 to validate our measurements of genome size from 2022, and we averaged measurements across the two years. Our sampling included 65 deciduous azaleas, of which 42 were from identified species growing in the field, 17 were naturally occurring hybrids whose assumed parentage was based on phenotypes intermediate between individuals of known taxonomic identity growing nearby, and six were from artificially generated hand crosses (Table S1). Hybrids represent natural experiments in trait covariation. Although our field sampling included multiple individuals identified as the same species, we have not averaged the trait values per species because taxonomic identification of deciduous azaleas is challenging even for taxonomic experts, with substantial evidence that there is rampant hybridization even among species differing in ploidy. In addition to naturally occurring plants, we also collected a variety of *Rhododendron* taxa from botanical gardens throughout the U.S., including the University of California Botanic Garden in Berkeley, CA, the Rhododendron Species Foundation Garden in Federal Way, WA, the Holden Arboretum in Kirtland, OH, the New York Botanic Garden in New York, NY, and the Davis Arboretum of Auburn University. Samples from the Rhododendron Species Foundation Garden were sampled in 2017, and all other samples were collected in 2022 and 2023. In total, sampled *Rhododendron* included representatives from four of the currently recognized *Rhododendron* subgenera: Tsutsusi, Rhododendron (including tropical Vireya), Pentanthera, and Hymenanthes (Xia et al. 2022). However, not all traits were measured on all samples; in particular, tropical Vireya were not measured for morphological traits, such as leaf thickness, water content, and LMA.

2.2-Genome size

To determine genome size by flow cytometry, we followed standard protocols for measuring genome size in plants (Dolezel et al. 2007; Pellicer and Leitch 2014). Approximately 50–100 mg of young and fresh leaf tissue was finely chopped over ice using a fresh razor blade along with fresh standard leaf material [*Zea mays* L., 1C = 2.71 pg; Lysak and Dolezel (1998)] in 2 ml ice-cold Galbraith's buffer (45 mM $MgCl_2$, 20 mM MOPS, 30 mM sodium citrate, 0.1% (v/v) Triton X-100, pH 7.0, (Galbraith et al. 1983)). Seeds of the plant standard were generously provided by the Institute of Experimental Botany, Czech Academy of Sciences. After filtering the homogenate through a 30-µm nylon mesh filter (CellTrics™, Sysmex), 50–100 µg/mL propidium iodide was added. Samples were incubated on ice for 15 minutes prior to analysis. Flow cytometry was performed using a BD Accuri C6 Flow Cytometer (BD Biosciences). For each unknown sample, at least 5000 nuclei were counted, with a coefficient of variation <5% for measured peaks. The 2C-value representing the genome size was determined as (Pellicer and Leitch 2014):

$$C_u = \frac{G1_u}{G1_s} \cdot C_s \text{ (equation 1)}$$

where C_u is the 2C DNA content of the unknown sample, C_s is the 2C DNA content of the standard, and $G1_u$ and $G1_s$ are the mean G1 peaks for the unknown sample and standard, respectively.

2.3-Leaf traits

For each plant sampled, we collected freshly cut shoots that had mature leaves, sampling these shoots in the early morning. Shoots were immediately sealed in humid plastic bags during transport back to the laboratory prior to sample processing. For each plant, we selected two leaves for analysis, both of which were measured for leaf thickness (T_L) in three locations using a digital thickness gauge (resolution: 0.01 mm; Mitutoyu 700-118-20), taking care to avoid prominent veins. One of these leaves was weighed for fresh mass, scanned for leaf area and shape, and dried for at least 72 hrs at 70°C for subsequent dry mass measurement (resolution: 0.001 g; Sartorius). We did not observe any leaves that were notably past the point of turgor loss, implying that the water content we measured

was within the range of physiological activity during the day. The other leaf was used for anatomical measurements. Approximately 1 cm^2 sections of leaves were cleared by incubating them at 70°C in a 1:1 solution of H_2O_2 (30% hydrogen peroxide) and CH_3COOH (100% acetic acid) for 24 hrs. The sections were then thoroughly rinsed in water, and their epidermises carefully separated from the layer of mesophyll and veins using a paintbrush. The epidermal layers were then stained with Safranin O (1% w/v in water) for 5-10 minutes, followed by a wash with water and a subsequent staining with Alcian Blue (1% w/v in 50% v/v ethanol) for 1 min and a rinse in 85% ethanol. The stained layers were then mounted onto microscope slides using CytoSeal (Fisher Scientific). Images were captured at varying magnifications (10x, 20x, or 40x) using a compound microscope equipped with a digital camera (Raspberry Pi High Quality Camera, Raspberry Pi Foundation). Both the abaxial and adaxial surfaces of the leaves were imaged for all species.

We used ImageJ (Rueden et al. 2017) to measure leaf anatomical traits. Guard cell length (l_g) was measured on at least 10 stomata per leaf from images taken at 40x magnification. The two-dimensional areas of epidermal pavement cells (A_{ec}) and stomatal guard cells (A_s) were measured by tracing the outlines of at least ten pavement cells or stomatal complexes (two guard cells) for each sample on 40x images. Stomatal (D_s) and epidermal pavement (D_{ec}) cell densities were measured on 20x or 40x images by counting all the cells of each cell type in a field of view and dividing by the area of the field of view. For most samples, the field of view was the entire image, but when the entire image was not in focus, only the image area in focus was used. We measured leaf vein density (D_v) as the total length of veins in an image divided by the dimensions of the image. To compare our anatomical measurements with previously published data for angiosperms, we used the dataset of l_g, D_s, and D_v, compiled by Jiang et al. (2023), which included data for 836 species from 126 families with 289 species that had both l_g and D_s measurements. Meristematic cell volumes as a function of genome size were taken from Šímová and Herben (2012). Using these measured volumes of meristematic cells, we approximated the maximum two-dimensional cross-sectional area of a spherical meristematic cell by calculating the cross-sectional area of a sphere with the same volume. We also estimated the maximum packing density of

spherical meristematic cells as the reciprocal of the cross-sectional area of a spherical meristematic cell (Théroux-Rancourt et al. 2021).

2.4-Data transformations and analyses

From measurements of leaf fresh mass (M_f), dry mass (M_d), and leaf area (A_L), we calculated the leaf mass per area (LMA) as:

$$LMA = \frac{M_d}{A_L} \text{ (equation 2)},$$

and leaf water content per unit area (W_{area}) was calculated as:

$$W_{area} = \frac{M_f - M_d}{18 \cdot A_L} \text{ (equation 3)},$$

where 18 represents the conversion from grams of water to moles of water.

Leaf density was calculated as:

$$LD = \frac{LMA}{T_L} \text{ (equation 4)},$$

where T_L is leaf thickness measured using a thickness gauge, as mentioned above.

Maximum stomatal conductance to water vapor was calculated from measurements of l_g and D_s (Franks and Beerling 2009):

$$g_{s,max} = \frac{\frac{d_{H_2O}}{v} \cdot D_s \cdot a_{max}}{d_p + \frac{\pi}{2}\sqrt{a_{max}/\pi}} \text{ (equation 5)},$$

where d_{H2O} is the diffusivity of water vapor in air (0.0000249 $m^2\ s^{-1}$), v is the molar volume of air normalized to 25 °C (0.0224 $m^3\ mol^{-1}$), d_p is the depth of the stomatal pore, and a_{max} is the maximum stomatal pore area. The depth of the stomatal pore, d_p, was assumed to be equal to the width of one guard cell, which was taken as $0.36 \cdot l_g$ (de Boer et al. 2016b). The maximum area of the open stomatal pore, a_{max}, was approximated as $\pi(p/2)^2$ where p is

stomatal pore length and was approximated as $l_g/2$. While both surfaces of the leaf are used for energy exchange, only one surface is used for gas exchange in hypostomatous leaves.

Maximum stomatal conductance, $g_{s,max}$, was used to calculate the mean leaf water residence time as:

$$\tau = \frac{W_{area}}{g_{s,max} \cdot VPD} \text{ (equation 6)}$$

with VPD = 1 kPa (Roddy et al. 2023). Because stomatal conductance under natural conditions is likely never near its anatomically defined maximum of $g_{s,max}$, this estimate of τ is likely much shorter than any τ encountered in nature. Nonetheless, it can be used to compare how W_{area} and leaf anatomy influence the temporal dynamics of resource turnover.

All statistical analyses were conducted in R (v. 4.1.2) (R Core Team 2018). Because the plants we sampled included putative interspecific interploidy hybrids, experimentally produced crosses with unclear taxonomic identity, and individuals sampled across species' ranges, we aggregated data to the individual plant level without reference to taxonomic rank (i.e. we did not calculate species means). Traits were log-transformed prior to most analyses because most traits exhibited a log-normal distribution . We used standard major axis (SMA) regression (R package 'smatr') to determine the scaling relationships between traits (Warton et al. 2012) and show confidence intervals around SMA regressions by bootstrapping the SMA regressions 1000 times. We used slope tests, implemented in 'smatr', to compare slopes, and we report *P*-values for whether the slopes are significantly different or not. Principal components analysis (PCA) using the R function 'princomp()' was used to determine multivariate trait covariation. Traits were log-transformed, centered, and scaled prior to calculating principal components. To partition variance explained among multiple factors, we used the function 'varpart()' in the R package 'vegan' (Oksanen et al. 2007).

To determine how T_L and cell size interact to influence $g_{s,max}$, we examined how traits covaried with regression residuals. We first used linear regression to determine the relationships between $g_{s,max}$ and T_L. The residuals of these regressions signify the variation

in $g_{s,max}$ and τ that is unexplained by T_L. We then tested whether these residuals were related to cell size. To minimize autocorrelation due to guard cell size being used in the calculation of $g_{s,max}$, we used instead epidermal cell size (A_{ec}), which nonetheless scaled significantly with l_g (R^2 = 0.36, P < 0.0001). There were significant negative relationships between epidermal cell size and the residuals of $g_{s,max}$ against T_L (R^2 = 0.12, P < 0.001) and τ against T_L (R^2 = 0.07, P < 0.01). To show the effects of cell size on the $g_{s,max}$ and τ versus T_L relationships, we calculated epidermal cell size isoclines for four epidermal cell sizes (400, 800, 1200, 1600 μm^2) by using the linear regression between the residuals and epidermal cell size; the residual values for each cell size was then added to the regression relationship of $g_{s,max}$ or τ versus T_L to generate the isoclines, which represent the average effect of cell size on the $g_{s,max}$ or τ versus T_L relationships (Figure 5b,d).

3-Results

3.1-Genome size diversity among Rhododendron

Consistent with previous studies of *Rhododendron* ploidy and genome size, our sampling found a range of 2C genome sizes among *Rhododendron* varying from 1.10 pg for *R. obtusum* to 3.90 pg for *R. leucogigas* (Table S1) (Khan et al. 2021; Hu et al. 2023). Among the section Pentanthera, there were three distinct groups that displayed 2C genome size values consistent with differences in ploidy and indicating likely interploidy hybrids (Figure S1; Table S1).

3.2-Scaling of genome size with cell sizes and packing densities

Among *Rhododendron* and angiosperms more broadly, the volumes and two-dimensional sizes of mature stomatal guard cells and epidermal pavement cells were always larger than the volumes and two-dimensional sizes of meristematic cells, and the packing densities of guard cells and epidermal cells were always lower than the packing densities of meristematic cells (Figure S2). Nonetheless, genome size was a significant predictor of guard cell volumes among *Rhododendron* (R^2 = 0.20, P < 0.0001) and angiosperms more broadly (R^2 = 0.38, P < 0.0001; Figure S2a). Though genome size explained only 20% of the variation in guard cell volume among *Rhododendron*, *Rhododendron* fell within the range of

trait space occupied by angiosperms more broadly (Figure 2a). The two-dimensional sizes of stomatal guard cells (R^2 = 0.20, P < 0.0001) and epidermal pavement cells (R^2 = 0.19, P < 0.0001) also scaled with genome size among *Rhododendron*, with stomatal guard cells being smaller than epidermal pavement cells (Figure S2b). Guard cell size also scaled significantly with genome size among a broader set of angiosperms (R^2 = 0.38, P < 0.0001; Figure S2b). Among angiosperms, stomatal density scaled negatively with genome size (R^2 = 0.23, P < 0.0001), but among *Rhododendron*, there was no significant relationship between stomatal density and genome size, though *Rhododendron* fell within the same range of trait space occupied by angiosperms (P = 0.1; Figure S2c). Epidermal cell packing density, which was higher than stomatal density, scaled negatively with genome size among genus *Rhododendron* (R^2 = 0.11, P < 0.05; Figure 2c). While vein density scaled negatively with genome size among angiosperms (R^2 = 0.30, P < 0.0001), there was no effect of genome size on vein density among *Rhododendron* (P = 0.14, Figure S2d).

3.3-Scaling among anatomical and morphological traits

Leaf dry mass per area (LMA) can be driven by variation in both leaf thickness and leaf density. Among *Rhododendron*, lamina thickness (T_L) scaled strongly with LMA (R^2 = 0.75, P < 0.0001; Figure 2a). Leaf density (LD) was almost as strongly linked to LMA as T_L (R^2 = 0.70, P < 0.0001; Figure 2b). Leaf thickness and leaf density also scaled positively with each other (R^2 = 0.22 P < 0.0001; Figure 2c). Because LMA can be influenced by both leaf thickness and leaf density, we partitioned the variance in LMA explained by these two variables. Among *Rhododendron*, leaf thickness explained 28% of the variation in LMA, and leaf density explained 19% of the variation in LMA. Jointly, leaf thickness and leaf density explained 49% of the variation in LMA, i.e. 49% of the variation in LMA is due to the covariation of LD and leaf T_L.

Because one of the major factors affecting leaf water residence time is leaf water content, we examined how leaf morphological traits scaled with W_{area} (Figure 3a,b). W_{area} scaled positively and significantly with T_L (R^2 = 0.85, P < 0.0001; Figure 3a) and LD (R^2 = 0.23, P < 0.0001; Figure 3b). However, cell size (here, guard cell length, l_g) was unrelated to both T_L and LD (Figure 3c,d).

3.4-Effects of anatomical and morphological traits on leaf function

Leaf water residence time (τ) is a function of both stomatal conductance (i.e. anatomical traits) and water content (i.e. morphological traits), such that increasing $g_{s,max}$ results in shorter τ (Figure S4) and increasing water content lengthens τ. τ scaled significantly and positively with both LMA (R^2 = 0.36, P < 0.001; Figure 4a) and LD (R^2 = 0.17, P < 0.001; Figure 4b). Though l_g and T_L can vary independently, both traits can impact leaf function. While there was no significant relationship between $g_{s,max}$ and T_L (Figure 5a), smaller cells lead to a higher $g_{s,max}$ for a given T_L (Figure 5b). Because thicker leaves have higher water content (Figure 3a), increasing T_L also leads to significantly longer τ (R^2 = 0.32, P < 0.001; Figure 5c). Furthermore, for a given T_L, reducing cell size shortens τ (Figure 5d).

In multivariate space, anatomical traits related to genome size-cell size allometry and morphological traits related to leaf construction costs were largely orthogonal to each other (Figure 6). Almost half (41%) of the variation among *Rhododendron* leaves was driven by the first principal component, which was driven by morphological traits that influence τ: T_L, LMA, and W_{area}. The second principal component, which explained 29% of the variation in leaf traits, was driven predominantly by anatomical traits associated with cell size: a tradeoff between large cells τ).

4-Discussion

Using *Rhododendron* as a case study, we show how cell size variation–due, in part, to variation in genome size–influences the construction and function of tissues and whole leaves even though anatomical traits related to cell size and morphological traits related to construction costs can vary independently. This analysis highlights how maximizing the leaf surface conductance, which increases A_{area}, is independent of the leaf traits that influence leaf durability and rates of resource turnover. By using closely related congeneric species to illuminate these relationships, this study provides a powerful test of the effects of cell size on leaf structure without the confounding effects of large ecological and evolutionary differences often implicit in interspecific comparisons among phylogenetically diverse taxa.

4.1-Effects of genome size on leaf anatomy

We found significant relationships between genome size, cell size, and cell packing density, consistent with previous analyses of phylogenetically diverse angiosperms (Beaulieu et al. 2007b; Beaulieu et al. 2008; Simonin and Roddy 2018; Roddy et al. 2020; Théroux-Rancourt et al. 2021) and among diverse species within habitats (Jiang et al. 2023). Despite exhibiting little interspecific variation in genome size compared to the variation among angiosperms, *Rhododendron* species exhibited significant relationships between genome size and anatomical traits. However, genome size was not as strong a predictor of cell packing densities as it was of cell sizes (Figure S2). That cells were always larger and packed less densely than the limits imposed by meristematic cells is consistent with the fundamental effects of genome size on minimum cell size but not mature cell size (Roddy et al. 2020). The presence of other cell types can also modify the effects of genome size on mature cell sizes and packing densities of any one tissue. For example, epidermal pavement cells fill the space unoccupied by stomata such that stomatal density is much lower than its potential maximum for a given stomatal size (Figure S2). Similarly, because multiple cell types occur throughout the leaf volume, there can be many combinations of cell sizes and packing densities among cell types (Roderick et al. 1999b; John et al. 2013).

4.2-Coordination among morphological and anatomical traits

There was strong coordination among morphological traits related to leaf construction. Because of the primacy of LMA in the LES, decomposing LMA into the factors driving it is important for understanding how leaves are built and function (Witkowski and Lamont 1991; Shipley 1995; Pyankov et al. 1999; John et al. 2017). Among *Rhododendron*, higher LMA was associated with both higher T_L and higher LD, and half of the variation in LMA was due to the covariation of LD and T_L (Figure 2). Among *Rhododendron*, T_L explained a greater proportion of variation in LMA (28%) than did LD (19%), in contrast to previous analyses of Mediterranean woody species, among which 45% of the variation in LMA was due to LD and 33% to T_L (De La Riva et al. 2016). Thus, increasing LMA in *Rhododendron* is due primarily to increasing thickness, either by larger cells typically associated with larger genome sizes or by additional layers of cells.

Because metabolism occurs in an aqueous environment and because water content influences hydraulic capacitance, higher water content links carbon economics and water relations (Roderick et al. 1999b; Roddy et al. 2019; Huang et al. 2020; Wang et al. 2022; Nadal et al. 2023). All else being equal, thicker leaves have more leaf volume in which to hold water, resulting in strong scaling relationships between T_L and W_{area} (Figure 3). However, cell size was unrelated to T_L, LD, or W_{area} (Figure 3), highlighting how variation at the level of the cell does not necessarily scale up to influence leaf-level variation.

4.3-Leaf construction and function from cells to whole leaves

Nonetheless, variation at the level of the cell can impact higher order processes, such as whole leaf structure and photosynthetic capacity, though these effects can be diffuse. While genome size has a pervasive effect on all leaf cell types (Théroux-Rancourt et al. 2021), tissues can be modified independently of genome size-cell size allometry either by varying cell expansion or because there are multiple cell types in the leaf (Figure 5). Individual cells can have thicker cell walls, increasing their mass at constant cell size, and cells can have various shapes that change the ratio of cell surface area to cell volume, ameliorating the negative effects of large cell volumes on diffusion (Théroux Rancourt et al. 2020; Treado et al. 2022). At the level of tissues, increasing thickness by adding more cell layers can influence diffusion and τ independently of cell size and shape. Similarly, at the level of the leaf, leaf thickness and mesophyll porosity can vary independently of cell size and cell packing density, allowing many leaf architectures to be built from the same cells (Théroux-Rancourt et al. 2021). For example, sun leaves and shade leaves on the same plant that have the same genome size can vary dramatically in leaf thickness, LMA, and W_{area}, resulting in different mesophyll structures for CO_2 diffusion and different photosynthetic rates (Théroux-Rancourt et al. 2023). Our results highlight how morphological traits related to leaf construction vary orthogonally to anatomical traits related to cell size (Figure 6).

However, this does not mean that cell size has no effect on whole-leaf structure and function. Previous work has shown how smaller, more densely packed stomata in the epidermis allow for higher leaf surface conductance to CO_2 (Franks and Beerling 2009; de Boer et al. 2012; Simonin and Roddy 2018). Once inside the leaf, CO_2 must diffuse through

the intercellular airspace and into the mesophyll cells. While smaller mesophyll cells allow for higher mesophyll surface area to be packed into a given leaf volume (Théroux-Rancourt et al. 2021), one of the major determinants of mesophyll conductance is leaf thickness (Roderick et al. 1999a; Earles et al. 2018). Because thinner leaves have a higher capacity for energy and matter exchange due to their higher ratio of surface area to volume, we predicted that realizing this potential would require smaller cells. Though T_L was unrelated to $g_{s,max}$, reducing cell size for a given T_L nonetheless resulted in a higher $g_{s,max}$ (Figure 5d).

Even more interesting were the effects of cell size on the mean leaf water residence time (τ). Though rarely measured, τ is an important and dynamic indicator of how rapidly leaf water content is replaced, providing a functional link between water content and stomatal dynamics (Nobel and Jordan 1983; Hunt and Nobel 1987; Farquhar and Cernusak 2005; Simonin et al. 2013; Roddy et al. 2018). The positive association between T_L and τ suggests that thicker, more durable leaves have slower rates of resource turnover. Though τ has not been part of the LES, our analysis highlights that traits such as LMA and T_L, which are associated with long LL, are also associated with slower rates of resource turnover (Reich 2014). Furthermore, because smaller cells elevate $g_{s,max}$, smaller cells allow for shorter τ even if T_L remains constant (Figure 5d). The development of the LES has largely ignored anatomical traits related to cell size (but see Shipley et al. 2006; Poorter et al. 2009), and previous attempts to link genome size to the LES have revealed no significant relationships (Beaulieu et al. 2007a). Our analysis clarifies how genome size-cell size variation influences whole-leaf construction and the LES by influencing $g_{s,max}$, A_{area}, and τ independently of T_L and LMA [Figure 5; Simonin and Roddy (2018); Roddy et al. (2020)].

Our analyses also clarify how functional tradeoffs can result from recurrent motifs in anatomical and morphological traits. Though anatomical and morphological traits varied orthogonally to each other, they resulted in a tradeoff between high $g_{s,max}$ and τ (Figure 6). The multivariate axis defined by the tradeoff between $g_{s,max}$ and τ is dominated by combinations of small cells and thin leaves (high $g_{s,max}$) versus large cells and thick leaves (lengthy τ). This covariation in cell size and leaf thickness is consistent with theory and data showing that the vein density that optimally supplies leaf transpiration occurs when the distance between adjacent veins is equal to the distance between veins and the

epidermis, i.e. vein densities should scale inversely with leaf thickness (Noblin et al. 2008). However, other analyses have shown that, under different functional demands, vein positioning may deviate from that predicted by optimal vein density (de Boer et al. 2016a). Selection on different functional requirements can drive variation in traits orthogonal to the tradeoff between $g_{s,max}$ and τ. For example, thick leaves with high LMA are often tougher, providing better mechanical defense against leaf damage and better thermal capacitance, which may be beneficial in certain environments (Leigh et al. 2012; de Boer et al. 2016a; Tserej and Feeley 2021). These leaves may also be long-lived, tough, and resistant to mechanical damage (Wright et al. 2004). Similarly, selection for increased CO_2 supply to the mesophyll may result in smaller cells even while selection for mechanical defense maintains constant T_L and LMA. Yet, while cell size traits and leaf morphological traits can vary independently of each other (Figures 3,5, and 6), our analyses show that cell size nonetheless influences higher-order leaf structure and function (Figure 5). In this way, cell size–and, indeed, genome size–may underlie these ecophysiological strategy axes, linking hydraulic, photosynthetic, and biomechanical functions, although there is substantial room for higher-level modification of leaf construction to accommodate a range of cell and genome sizes (Pyankov et al. 1999; Shipley et al. 2006; Roddy et al. 2020; Nadal et al. 2023). That these relationships exist among close relatives further reiterates the effects of cell size on leaf construction and ecological performance.

Author Contributions

A.B.R. and A.D. conceptualized the study. A.D., M.W., S.P., J.P., C.H., P.T., C.R., J.M., Y.-D. A., G.-F. J., and A.B.R. collected the data. A.D., K.A.S., and A.B.R. analyzed the data. A.B.R., A.D., and K.A.S. wrote the manuscript with input from all coauthors.

Acknowledgments

We thank M. Hatchadourian and C. Lyman of the New York Botanical Garden, H. Forbes of the University of California Botanical Garden, and S. Hootman of the Rhododendron Species Botanical Garden for facilitating access to and providing plant material. This work was supported by grants DEB-1838327 to K.A.S. and A.B.R. and CMMI-2029756 to A.B.R. from the U.S. National Science Foundation.

Data availability statement

The data that supports the findings of this study are available in the supplementary material of this article.

References

Bazzaz FA, Chiariello NR, Coley PD, Pitelka LF (1987) Allocating resources to reproduction and defense. BioScience 37: 58–67

Beaulieu JM, Leitch IJ, Knight CA (2007a) Genome size evolution in relation to leaf strategy and metabolic rates revisited. Annals of Botany 99: 495–505

Beaulieu JM, Leitch IJ, Patel S, Pendharkar A, Knight CA (2008) Genome size is a strong predictor of cell size and stomatal density in angiosperms. New Phytologist 179: 975–986

Beaulieu JM, Moles AT, Leitch IJ, Bennett MD, Dickie JB, Knight CA (2007b) Correlated evolution of genome size and seed mass. New Phytologist 173: 422–437

Bonan GB, Williams M, Fisher RA, Oleson KW (2014) Modeling stomatal conductance in the earth system: linking leaf water-use efficiency and water transport along the soil–plant–atmosphere continuum. Geosci Model Dev 7: 2193–2222

Borsuk A, Roddy AB, Théroux-Rancourt G, Brodersen CR (2022) Structural organization of the spongy mesophyll. New Phytologist 234: 946–960

Boyce CK, Lee J-E (2010) An exceptional role for flowering plant physiology in the expansion of tropical rainforests and biodiversity. Proceedings of the Royal Society B: Biological Sciences 277: 3437–3443

Chapin FS (1989) The cost of tundra plant structures: evaluation of concepts and currencies. The American Naturalist 133: 1–19

de Boer HJ, Drake PL, Wendt E, Price CA, Schulze E-D, Turner NC, Nicolle D, Veneklaas EJ (2016a) Apparent Overinvestment in Leaf Venation Relaxes Leaf Morphological Constraints on Photosynthesis in Arid Habitats. Plant Physiology 172: 2286–2299

de Boer HJ, Eppinga MB, Wassen MJ, Dekker SC (2012) A critical transition in leaf evolution facilitated the Cretaceous angiosperm revolution. Nature Communications 3: 1221

de Boer HJ, Price CA, Wagner-Cremer F, Dekker SC, Franks PJ, Veneklaas EJ (2016b) Optimal allocation of leaf epidermal area for gas exchange. New Phytologist 210: 1219–1228

De KK, Saha A, Tamang R, Sharma B (2010) Investigation on relative genome sizes and ploidy levels of Darjeeling-Himalayan Rhododendron species using flow cytometer. Indian Journal of Biotechnology 9: 64–68

De La Riva EG, Olmo M, Poorter H, Ubera JL, Villar R (2016) Leaf Mass per Area (LMA) and Its Relationship with Leaf Structure and Anatomy in 34 Mediterranean Woody Species along a Water Availability Gradient. PLoS ONE 11: e0148788

Dolezel J, Greilhuber J, Suda J (2007) Estimation of nuclear DNA content in plants using flow cytometry. Nature Protocols 2: 2233–44

Earles JM, Théroux-Rancourt G, Roddy AB, Gilbert ME, McElrone AJ, Brodersen CR (2018) Beyond porosity: 3D leaf intercellular airspace traits that impact mesophyll conductance. Plant Physiology 178: 148–162

Farquhar GD, Cernusak LA (2005) On the isotopic composition of leaf water in the non-steady state. Functional Plant Biol 32: 293–303

Franks PJ, Beerling DJ (2009) Maximum leaf conductance driven by CO_2 effects on stomatal size and density over geologic time. Proceedings of the National Academy of Sciences 106: 10343–10347

Franks PJ, Berry JA, Lombardozzi DL, Bonan GB (2017) Stomatal Function across Temporal and Spatial Scales: Deep-Time Trends, Land-Atmosphere Coupling and Global Models. Plant Physiology 174: 583–602

Galbraith DR, Harkins KR, Maddox JM, Ayres NM, Sharma DP, Firoozabady E (1983) Rapid Flow Cytometric Analysis of the Cell Cycle in Intact Plant Tissues | Science. Science 220: 1049–1051

Hu L, Tate JA, Gardiner SE, MacKay M (2023) Ploidy variation in Rhododendron subsection Maddenia and its implications for conservation. AoB PLANTS 15: plad016

Huang H, Ran J, Ji M, Wang Z, Dong L, Hu W, Deng Y, Hou C, Niklas KJ, Deng J (2020) Water content quantitatively affects metabolic rates over the course of plant ontogeny. New Phytologist 228: 1524–1534

Hunt ERJr, Nobel PS (1987) Non-steady state water flow for three desert perennials with different capacitances. Australian Journal of Plant Physiology 14: 363–375

Jiang G-F, Li S-Y, Dinnage R, Cao K-F, Simonin KA, Roddy AB (2023) Diverse mangroves deviate from other angiosperms in their genome size, leaf cell size and cell packing density relationships. Annals of Botany mcac151

John GP, Scoffoni C, Buckley TN, Villar R, Poorter H, Sack L (2017) The anatomical and compositional basis of leaf mass per area. Ecology Letters 20: 412–425

John GP, Scoffoni C, Sack L (2013) Allometry of cells and tissues within leaves. American Journal of Botany 100: 1936–1948

Jones JR, Ranney TG, Lynch NP, Krebs SL (2007) Ploidy Levels and Relative Genome Sizes of Diverse Species, Hybrids, and Cultivars of Rhododendron. Journal of the American Rhododendron Society 61: 220–227

Khan G, Nolzen J, Schepker H, Albach DC (2021) Incongruent phylogenies and their implications for the study of diversification, taxonomy, and genome size evolution of Rhododendron. American Journal of Botany 108: 1957–1981

Kikuzawa K, Lechowicz MJ (2006) Toward synthesis of relationships among leaf longevity, instantaneous photosynthetic rate, lifetime leaf carbon gain, and the gross primary production of forests. The American Naturalist 168: 373–383

Kikuzawa K, Lechowicz MJ (2011) Ecology of leaf longevity. Springer Science & Business Media

Kikuzawa K, Lechowicz MJ (2018) Leaf Photosynthesis Integrated over Time. In: Adams Iii WW, Terashima I (eds) The Leaf: A Platform for Performing Photosynthesis. Springer International Publishing, Cham, pp. 473–492

Leigh A, Sevanto S, Ball MC, Close JD, Ellsworth DS, Knight CA, Nicotra AB, Vogel S (2012) Do thick leaves avoid thermal damage in critically low wind speeds? New Phytologist 194: 477–487

Lloyd J, Bloomfield K, Domingues TF, Farquhar GD (2013) Photosynthetically relevant foliar traits correlating better on a mass vs an area basis: of ecophysiological relevance or just a case of mathematical imperatives and statistical quicksand? New Phytologist 199: 311–321

Lysak MA, Dolezel J (1998) Estimation of nuclear DNA content in Sesleria (Poaceae). Caryologia 51: 123–132

Nadal M, Clemente-Moreno MJ, Perera-Castro AV, Roig-Oliver M, Onoda Y, Gulías J, Flexas J (2023) Incorporating pressure–volume traits into the leaf economics spectrum. Ecology Letters 26: 549–562

Nobel PS, Jordan PW (1983) Transpiration stream of desert species: resistances and capacitances for a C3, a C4, and a CAM plant. Journal of Experimental Botany 34: 1379–1391

Noblin X, Mahadevan L, Coomaraswamy IA, Weitz DA, Holbrook NM, Zwieniecki MA (2008) Optimal vein density in artificial and real leaves. Proceedings of the National Academy of Sciences 105: 9140–9144

Oksanen J, Kindt R, Legendre P, O'Hara B, Stevens MHH, Oksanen MJ, Suggests M (2007) The vegan package. Community ecology package 10: 719

Onoda Y, Wright IJ, Evans JR, Hikosaka K, Kitajima K, Niinemets Ü, Poorter H, Tosens T, Westoby M (2017) Physiological and structural tradeoffs underlying the leaf economics spectrum. New Phytologist 214: 1447–1463

Osnas JLD, Lichstein JW, Reich PB, Pacala SW (2013) Global Leaf Trait Relationships: Mass, Area, and the Leaf Economics Spectrum. Science 340: 741–744

Pellicer J, Leitch IJ (2014) The Application of Flow Cytometry for Estimating Genome Size and Ploidy Level in Plants. In: Besse P (ed) Molecular Plant Taxonomy: Methods and Protocols. Humana Press, Totowa, NJ, pp. 279–307

Poorter H, Niinemets Ü, Poorter L, Wright IJ, Villar R (2009) Causes and consequences of variation in leaf mass per area (LMA): a meta-analysis. New Phytologist 182: 565–588

Poorter H, Remkes C, Lambers H (1990) Carbon and nitrogen economy of 24 wild species differing in relative growth rate. Plant physiology 94: 621–627

Pyankov VI, Kondratchuk AV, Shipley B (1999) Leaf structure and specific leaf mass: the alpine desert plants of the Eastern Pamirs, Tadjikistan. The New Phytologist 143: 131–142

R Core Team (2018) R: a language and environment for statistical computing. R Foundation for Statistical Computing, Vienna, Austria

Reich PB (2014) The world-wide 'fast-slow' plant economics spectrum: a traits manifesto. Journal of Ecology 102: 275–301

Reich P, Walters M, Ellsworth D (1992) Leaf life-span in relation to leaf, plant, and stand characteristics among diverse ecosystems. Ecological monographs 62: 365–392

Roddy AB, Guilliams CM, Fine PVA, Mambelli S, Dawson TE, Simonin KA (2023) Flowers are leakier than leaves but cheaper to build. New Phytologist 239: 2076–2082

Roddy AB, Jiang G.-F., Cao K-F, Simonin KA, Brodersen CR (2019) Hydraulic traits are more diverse in flowers than in leaves. New Phytologist 223: 193–203

Roddy AB, Simonin KA, McCulloh KA, Brodersen CR, Dawson TE (2018) Water relations of Calycanthus flowers: Hydraulic conductance, capacitance, and embolism resistance. Plant, Cell & Environment 41: 2250–2262

Roddy AB, Théroux-Rancourt G, Abbo T, Benedetti JW, Brodersen CR, Castro M, Castro S, Gilbride AB, Jensen B, Jiang G-F, Perkins JA, Perkins SD, Loureiro J, Syed Z, Thompson RA, Kuebbing SE, Simonin KA (2020) The scaling of genome size and cell size limits maximum rates of photosynthesis with implications for ecological strategies. International Journal of Plant Sciences 181: 75–87

Roderick ML, Berry SL, Noble IR, Farquhar GD (1999a) A theoretical approach to linking the composition and morphology with the function of leaves. Functional Ecology 13: 683–695

Roderick ML, Berry SL, Saunders AR, Noble IR (1999b) On the relationship between the composition, morphology and function of leaves. Functional Ecology 13: 696–710

Rueden CT, Schindelin J, Hiner MC, DeZonia BE, Walter AE, Arena ET, Eliceri KW (2017) ImageJ2: ImageJ for the next generation of scientific image data. BMC Bioinformatics 18: 529

Schepper SD, Leus L, Mertens M, Bockstaele EV, Loose MD, Debergh P, Heursel J (2001) Flow Cytometric Analysis of Ploidy in Rhododendron (subgenus Tsutsusi). HortScience 36: 125–127

Shipley B (1995) Structured Interspecific Determinants of Specific Leaf Area in 34 Species of Herbaceous Angiosperms. Functional Ecology 9: 312–319

Shipley B, Lechowicz MJ, Wright I, Reich PB (2006) Fundamental Tradeoffs Generating the Worldwide Leaf Economics Spectrum. Ecology 87: 535–541

Shrestha N, Wang Z, Su X, Xu X, Lyu L, Liu Y, Dimitrov D, Kennedy JD, Wang Q, Tang Z, al et (2018) Global patterns of *Rhododendron* diversity: The role of evolutionary time and diversification rates. Global Ecology and Biogeography 27: 913–924

Simonin KA, Roddy AB (2018) Genome downsizing, physiological novelty, and the global dominance of flowering plants. PLoS Biology 16: e2003706

Simonin KA, Roddy AB, Link P, Apodaca R, Tu KP, Hu J, Dawson TE, Barbour MM (2013) Isotopic composition of transpiration and rates of change in leaf water isotopologue storage in response to environmental variables. Plant, Cell & Environment 36: 2190–2206

Šímová I, Herben T (2012) Geometrical constraints in the scaling relationships between genome size, cell size and cell cycle length in herbaceous plants. Proceedings of the Royal Society B: Biological Sciences 279: 867–875

Théroux-Rancourt G, Herrera JC, Voggeneder K, De Berardinis F, Luijken N, Nocker L, Savi T, Scheffknecht S, Schneck M, Tholen D (2023) Analyzing anatomy over three dimensions unpacks the differences in mesophyll diffusive area between sun and shade Vitis vinifera leaves. AoB PLANTS 15: plad001

Théroux-Rancourt G, Roddy AB, Earles JM, Gilbert ME, Zwieniecki MA, Boyce CK, Tholen D, McElrone AJ, Simonin KA, Brodersen CR (2021) Maximum CO_2 diffusion inside leaves is limited by the scaling of cell size and genome size. Proceedings of the Royal Society B 288: 20203145

Théroux Rancourt G, Voggeneder K, Tholen D (2020) Shape matters: the pitfalls of analyzing mesophyll anatomy. New Phytol 225: 2239–2242

Treado JD, Roddy AB, Théroux-Rancourt G, Zhang L, Ambrose C, Brodersen CR, Shattuck MD, O'Hern CS (2022) Localized growth and remodelling drives spongy mesophyll morphogenesis. Journal of The Royal Society Interface 19: 20220602

Tserej O, Feeley KJ (2021) Variation in leaf temperatures of tropical and subtropical trees are related to leaf thermoregulatory traits and not geographic distributions. Biotropica 53: 868–878

Violle C, Navas M-L, Vile D, Kazakou E, Fortunel C, Hummel I, Garnier E (2007) Let the concept of trait be functional! Oikos 116: 882–892

Wang Z, Huang H, Wang H, Peñuelas J, Sardans J, Niinemets Ü, Niklas KJ, Li Y, Xie J, Wright IJ (2022) Leaf water content contributes to global leaf trait relationships. Nat Commun 13: 5525

Warton DI, Duursma RA, Falster DS, Taskinen S (2012) smatr 3—an R package for estimation and inference about allometric lines. Methods in Ecology and Evolution 3: 257–259

Westoby M, Reich PB, Wright IJ (2013) Understanding ecological variation across species: area-based vs mass-based expression of leaf traits. New Phytologist 199: 322–323

Witkowski ETF, Lamont BB (1991) Leaf specific mass confounds leaf density and thickness. Oecologia 88: 486–493

Wright IJ, Reich PB, Westoby M, Ackerly DD, Baruch Z, Bongers F, Cavender-Bares J, Chapin T, Cornelissen JH, Diemer M, others (2004) The worldwide leaf economics spectrum. Nature 428: 821

Xia X-M, Yang M-Q, Li C-L, Huang S-X, Jin W-T, Shen T-T, Wang F, Li X-H, Yoichi W, Zhang L-H, Zheng Y-R, Wang X-Q (2022) Spatiotemporal evolution of the global species diversity of *Rhododendron*. Molecular Biology and Evolution 39: msab314

Figure legends

Figure 1. Conceptual diagram showing how two primary traits influencing leaf structure and metabolic capacity–cell size and leaf thickness–can vary independently of each other.

Figure 2. Relationships between leaf thickness (T_L), leaf density (LD), and leaf mass per area (LMA) among *Rhododendron*. Both T_L and LD can influence LMA; among *Rhododendron* species, 28% of the variation in LMA is due to T_L, 19% of the variation in LMA is due to LD, and 49% of the variation in LMA is due to the covariation among T_L and LD. Pink lines and shading represent standard major axis regressions and 95% confidence intervals. Points are colored according to clade, and the relationships among clades in genus *Rhododendron* are shown.

Figure 3. The relationships among lamina thickness (T_L), leaf density (LD), leaf water content per unit area (W_{area}), and guard cell length (l_g). (a,b) W_{area} scales positively with T_L and LD. (c,d) There is no relationship between l_g and either T_L or LD. Pink lines and shading represent standard major axis regressions and 95% confidence intervals. Points are colored according to clade (see Figure 2).

Figure 4. Longer mean leaf water residence times (τ) are associated with higher (a) leaf mass per area (LMA) and higher (b) leaf density (LD). Pink lines and shading represent standard major axis regressions and 95% confidence intervals. Points are colored according to clade (see Figure 2).

Figure 5. Both cell size and leaf morphology influence leaf functional traits. (a) Leaf thickness (T_L) is unrelated to maximum leaf surface conductance ($g_{s,max}$). (b) However, reducing cell size for a given T_L elevates $g_{s,max}$. (c) Thicker leaves are associated with longer leaf water residence times (τ). (d) For a given T_L, reducing cell size shortens τ. In (b,d), yellow-red lines indicate cell size isoclines with numbers adjacent to lines indicating the 2D epidermal cell areas (A_{ec}). See methods for how cell size isoclines were calculated from the residuals of the bivariate relationships in (a,c). Pink lines and shading represent standard major axis regressions and 95% confidence intervals, with points colored according to clade (see Figure 2).

Figure 6. Principal components analysis of leaf traits among *Rhododendron* taxa shows that anatomical traits related to cell sizes and cell packing densities are largely orthogonal to morphological traits related to water content and dry mass investment. Trait loading vectors are colored according to trait type: anatomical traits related to cell size and packing density (blue), morphological traits related to water content and dry mass investment (orange), and physiological traits quantifying potential rates of resource flux and turnover (black). Cartoon cross-sections of leaves in each quadrant illustrate the combinations of anatomical and morphological traits associated with leaves that would occur in that quadrant. Note that leaf thickness (T_L), LMA, and W_{area} all have similar loadings.

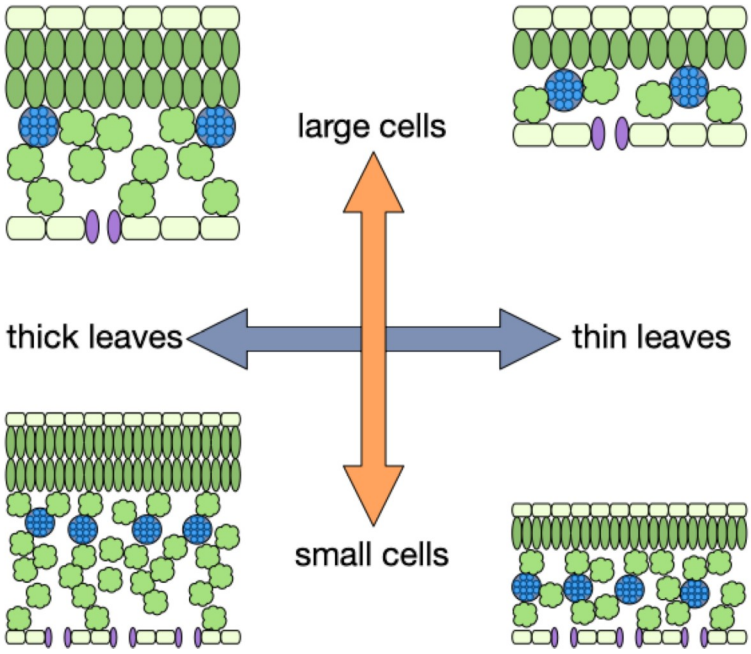

Figure 1. Conceptual diagram showing how two primary traits influencing leaf structure and metabolic capacity–cell size and leaf thickness–can vary independently of each other.

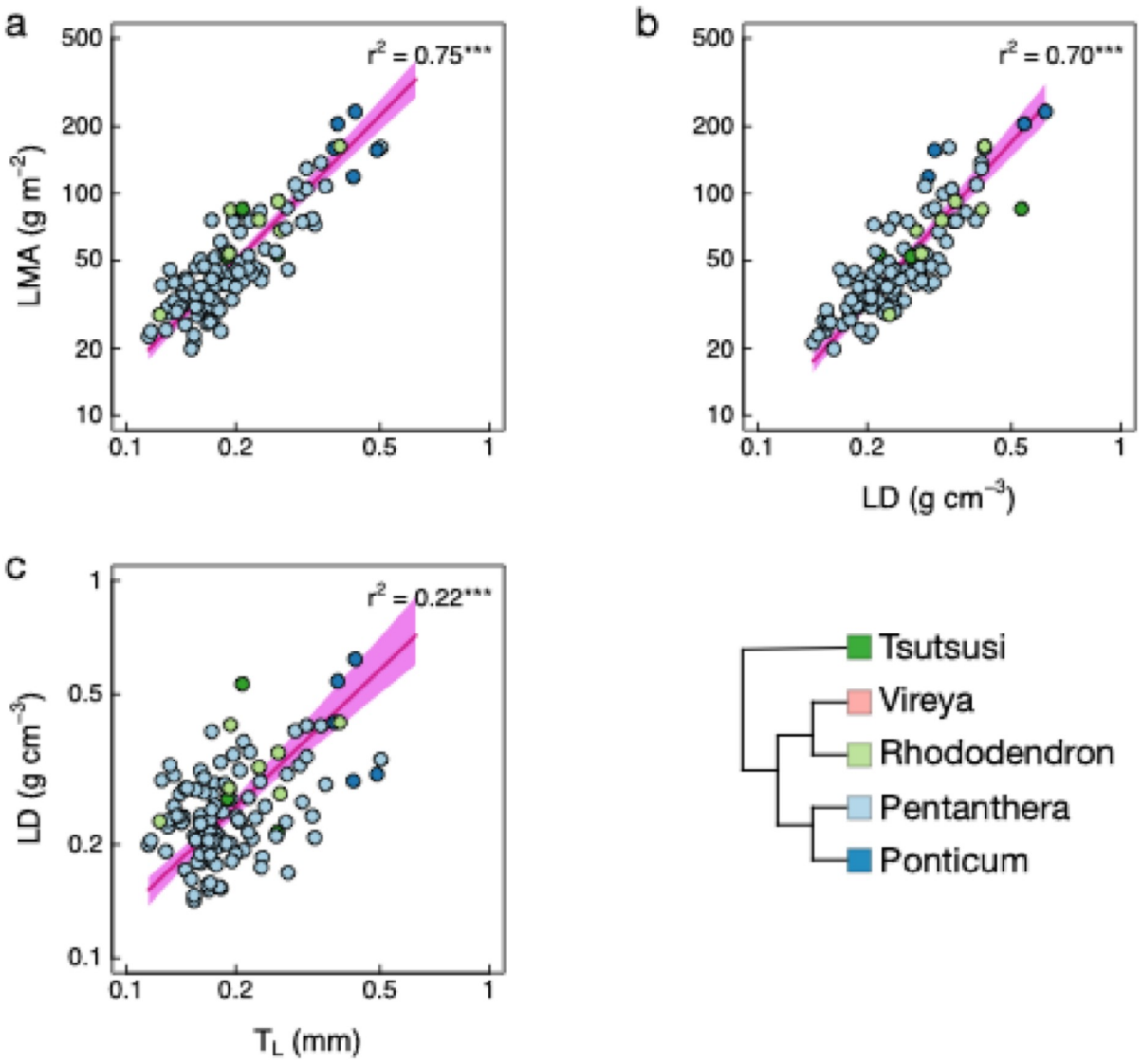

Figure 2. Relationships between leaf thickness (T_L), leaf density (LD), and leaf mass per area (LMA) among *Rhododendron*. Both T_L and LD can influence LMA; among Rhododendron species, 28% of the variation in LMA is due to T_L, 19% of the variation in LMA is due to LD, and 49% of the variation in LMA is due to the covariation among T_L and LD. Pink lines and shading represent standard major axis regressions and 95% confidence intervals. Points are colored according to clade, and the relationships among clades in genus *Rhododendron* are shown.

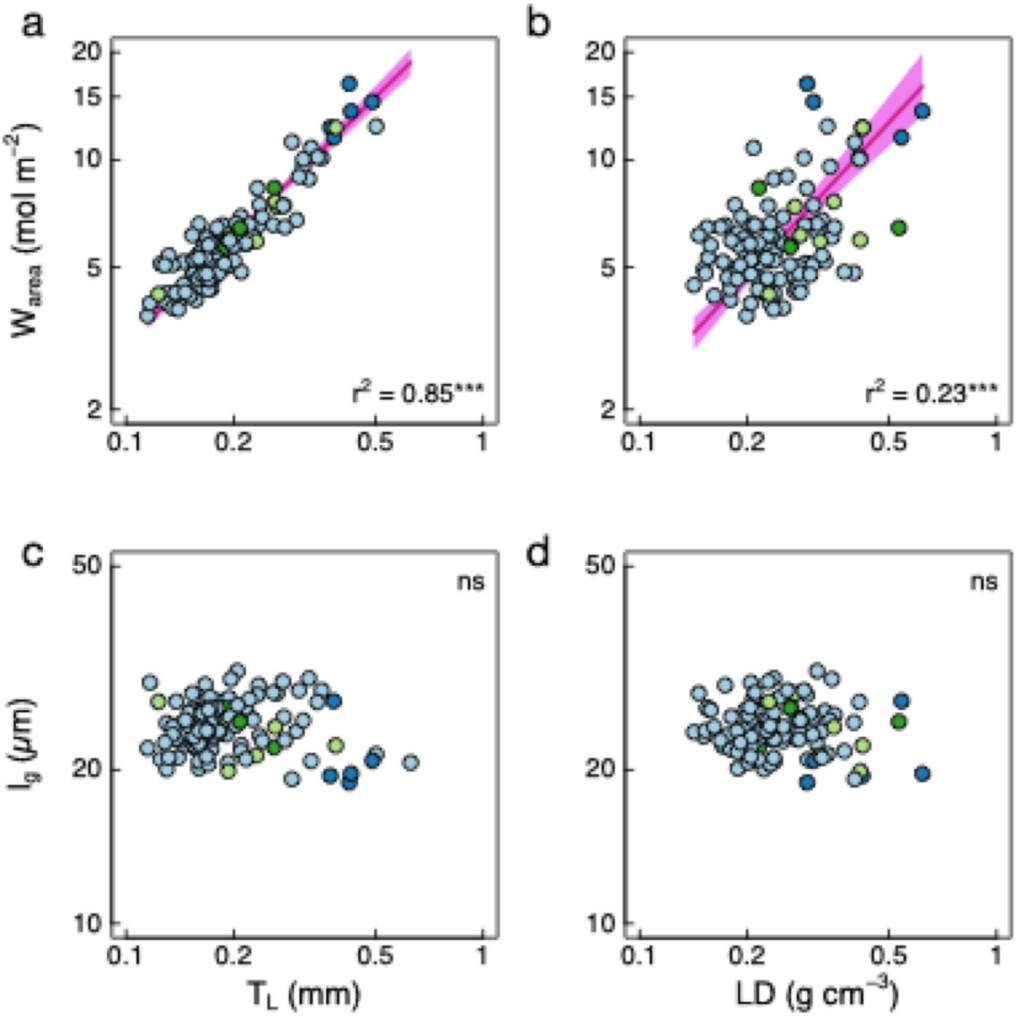

Figure 3. The relationships among lamina thickness (T_L), leaf density (LD), leaf water content per unit area (W_{area}), and guard cell length (l_g). (a,b) Warea scales positively with TL and LD. (c,d) There is no relationship between l_g and either T_L or LD. Pink lines and shading represent standard major axis regressions and 95% confidence intervals. Points are colored according to clade (see Figure 2).

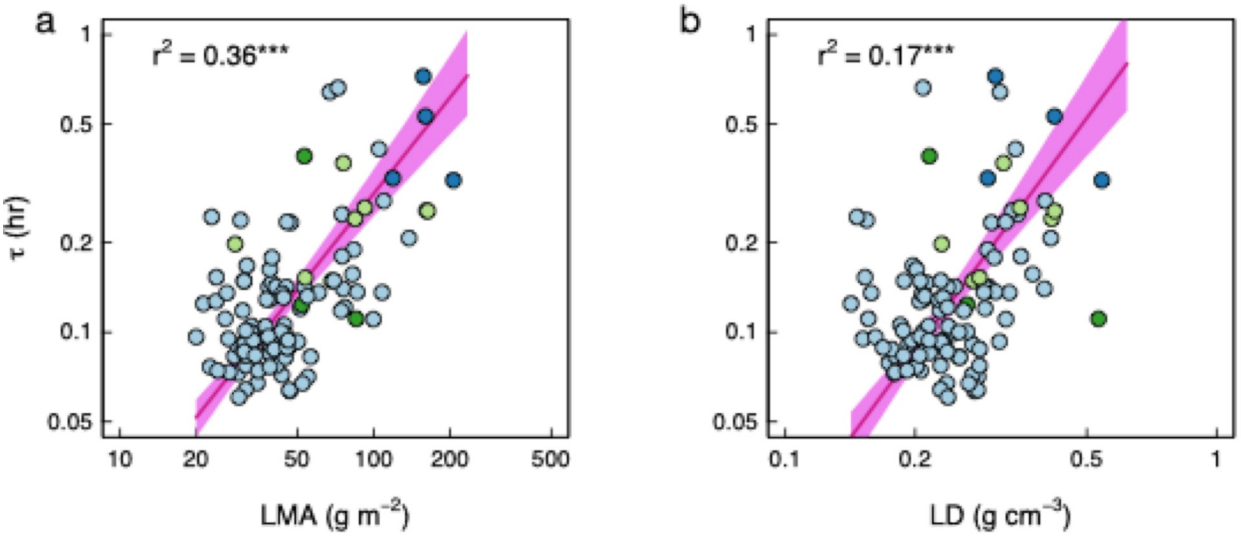

Figure 4. Longer mean leaf water residence times (τ) are associated with higher (a) leaf mass per area (LMA) and higher (b) leaf density (LD). Pink lines and shading represent standard major axis regressions and 95% confidence intervals. Points are colored according to clade (see Figure 2).

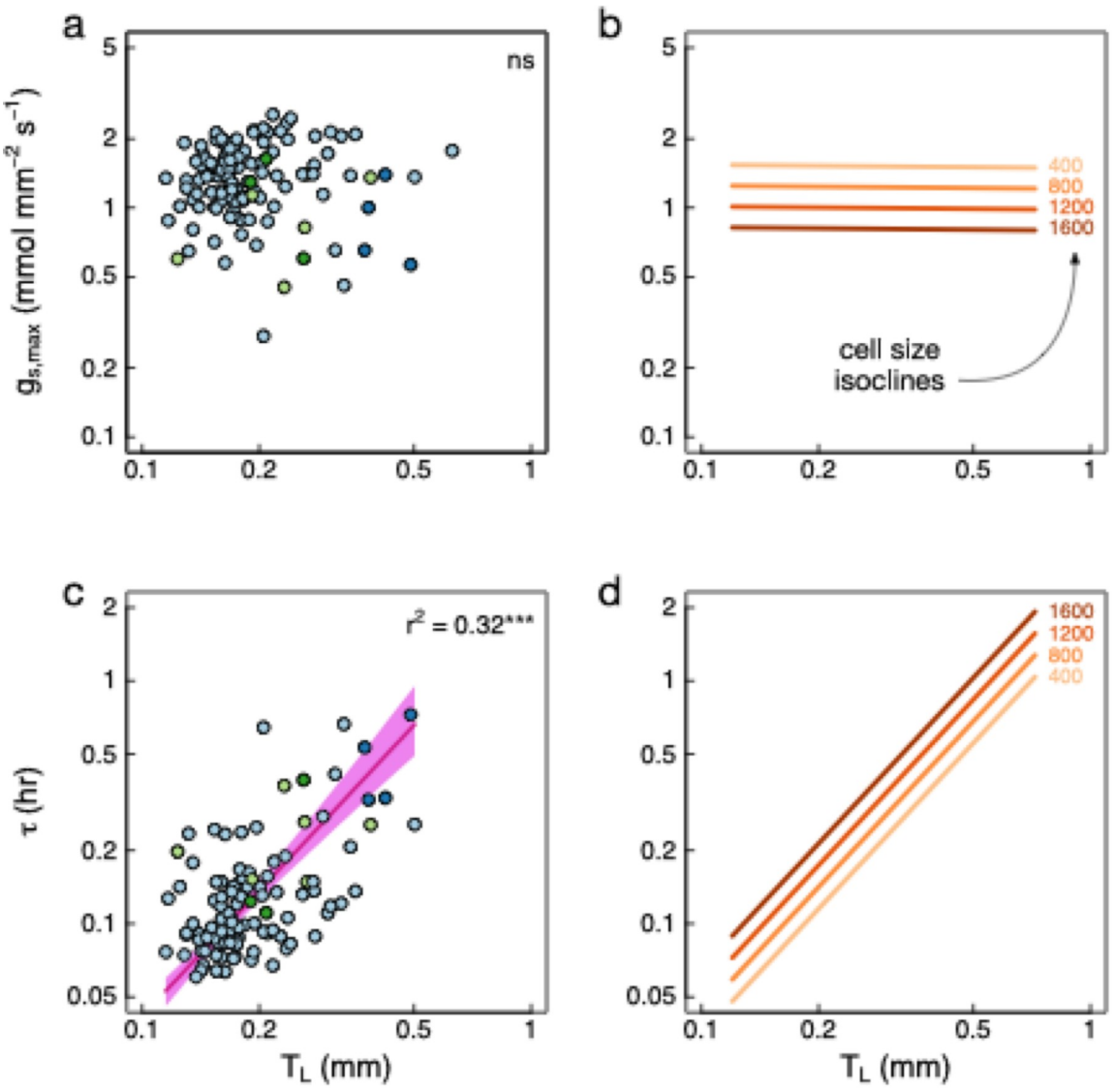

Figure 5. Both cell size and leaf morphology influence leaf functional traits. (a) Leaf thickness (T_L) is unrelated to maximum leaf surface conductance ($g_{s,max}$). (b) However, reducing cell size for a given T_L elevates $g_{s,max}$. (c) Thicker leaves are associated with longer leaf water residence times (τ). (d) For a given T_L, reducing cell size shortens τ. In (b,d), yellow-red lines indicate cell size isoclines with numbers adjacent to lines indicating the 2D epidermal cell areas (A_{ec}). See methods for how cell size isoclines were calculated from the residuals of the bivariate relationships in (a,c). Pink lines and shading represent standard major axis regressions and 95% confidence intervals, with points colored according to clade (see Figure 2).

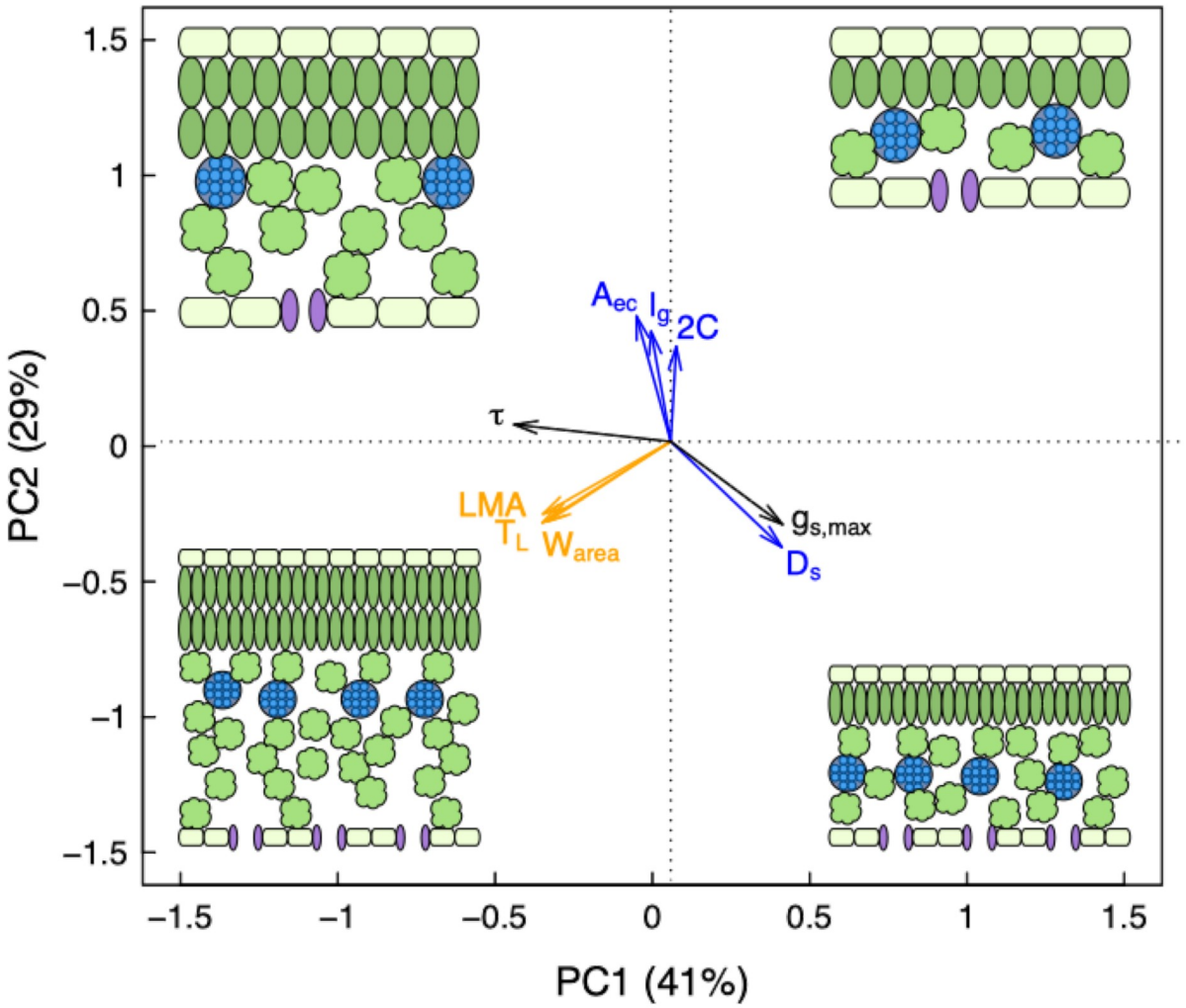

Figure 6. Principal components analysis of leaf traits among *Rhododendron* taxa shows that anatomical traits related to cell sizes and cell packing densities are largely orthogonal to morphological traits related to water content and dry mass investment. Trait loading vectors are colored according to trait type: anatomical traits related to cell size and packing density (blue), morphological traits related to water content and dry mass investment (orange), and physiological traits quantifying potential rates of resource flux and turnover (black). Cartoon cross-sections of leaves in each quadrant illustrate the combinations of

anatomical and morphological traits associated with leaves that would occur in that quadrant. Note that leaf thickness (T_L), LMA, and W_{area} all have similar loadings.